Protein roadblocks and helix discontinuities are barriers to the initiation of mismatch repair

Anna Pluciennik[†] and Paul Modrich[†‡§]

[†]Department of Biochemistry and [‡]Howard Hughes Medical Institute, Box 3711, Duke University Medical Center, Durham, NC 27710

Contributed by Paul Modrich, June 1, 2007 (sent for review May 21, 2007)

The hemimethylated d(GATC) sequence that directs *Escherichia coli* mismatch repair can reside on either side of a mismatch at a separation distance of 1,000 bp or more. Initiation of repair involves the mismatch-, MutS-, and MutL-dependent activation of MutH endonuclease, which incises the unmethylated strand at the d(GATC) sequence, with the ensuing strand break serving as the loading site for the appropriate 3′-to-5′ or 5′-to-3′ excision system. However, the mechanism responsible for the coordinated recognition of the mismatch and a hemimodified d(GATC) site is uncertain. We show that a protein roadblock ($EcoRI_{E111Q}$, a hydrolytically defective form of EcoRI endonuclease) placed on the helix between the two DNA sites inhibits MutH activation by 70–80% and that events that escape inhibition are attributable, at least in part, to diffusion of $EcoRI_{E111Q}$ away from its recognition site. We also demonstrate that a double-strand break located within the shorter path linking the mismatch and a d(GATC) site in a circular heteroduplex abolishes MutH activation, whereas a double-strand break within the longer path is without effect. These findings support the idea that initiation of mismatch repair involves signaling along the helix contour.

DNA repair | genetic stability | signaling

Mismatch repair is a conserved process that corrects biosynthetic errors and ensures the fidelity of homologous genetic recombination. Eleven activities have been implicated in *Escherichia coli* methyl-directed mismatch repair that has been reconstituted in a purified system. The reaction depends on MutS, MutL, MutH, DNA helicase II (MutU/UvrD), single-stranded DNA-binding protein, exonuclease I, exonuclease VII, exonuclease X, RecJ exonuclease, DNA polymerase III holoenzyme, and DNA ligase (1–4). The strand specificity necessary for replication error correction by this system is based on the transient absence of d(GATC) methylation in newly synthesized DNA (5).

Repair is initiated via mismatch recognition by MutS (6), which recruits MutL to the heteroduplex in a mismatch- and ATP-dependent fashion (7, 8). Assembly of the MutL–MutS–heteroduplex complex is sufficient to activate MutH endonuclease, which incises the unmethylated strand of a hemimethylated d(GATC)-strand signal (9) that may reside either 3′ or 5′ to the mismatch at distances of as much as 1 kb or more (2). MutS and MutL also activate DNA helicase II, which is loaded at the MutH strand break in an orientation-dependent manner, so that helix unwinding proceeds toward the mismatch (10). That portion of the incised strand displaced in this manner is degraded by a single-stranded exonuclease, resulting in mismatch removal. When the MutH nick is 3′ to the mismatch, the single-stranded hydrolytic requirement can be met by exonuclease I, exonuclease VII, or exonuclease X, and, when the nick is 5′ to the mispair, either exonuclease VII or RecJ will suffice in this regard (2–4). The mechanism responsible for action at a distance during mismatch repair is poorly understood, but the bidirectional excision capability presumably requires establishment of the relative orientation of the mismatch and the MutH-generated strand break at the d(GATC)-strand signal.

Three models have been proposed to explain interaction of the two DNA sites involved in mismatch repair. One invokes movement of MutS or the MutL–MutS complex along the helix between the mismatch and the strand signal (11–13), a second posits mismatch recognition by MutS as a trigger for polymerization of a second protein along the helix between the two DNA sites (11), and the third attributes interaction of the two sites to a DNA-looping mechanism (14, 15). Several laboratories have demonstrated that, when challenged with ATP, MutS homologs leave a mismatch by movement along the helix contour, and evidence for movement of the MutL–MutS homolog complex along DNA also is available (reviewed in refs. 16–18). However, there is no proof that movement in this manner is involved in signaling between the mismatch and the strand signal that directs repair. There also is no evidence for involvement of protein polymerization along the helix in mediating mismatch–strand signal interaction. The finding that a mismatch on one oligonucleotide duplex can activate MutS- and MutL-dependent MutH cleavage of a d(GATC) sequence located on a second duplex is consistent with the DNA-looping model (14, 15), but this reaction is inefficient compared with MutH activation in cis (9).

In the study described here, we tested these models in the *E. coli* repair system by placing a high-affinity, site-specific DNA-binding protein between the mismatch and the d(GATC)-strand signal. Our results show that a helix-bound protein roadblock substantially inhibits MutH activation. By using circular heteroduplexes, we also demonstrate that a helix disruption within the shorter path linking the mismatch and the d(GATC) abolishes MutH activation, whereas a discontinuity within the longer path has no effect. These findings strongly suggest that signaling along the helix between the mismatch and d(GATC) site is required for the initiation of *E. coli* mismatch repair.

Results

$EcoRI_{E111Q}$ Experimental System. EcoRI endonuclease with a Gln substitution for Glu111 ($EcoRI_{E111Q}$) is a hydrolytically defective form of the enzyme that binds to d(GAATTC) recognition sites with an affinity of 10^{13} M^{-1} at 150 mM NaCl (19). To analyze potential roadblock effects of this protein on the initiation of mismatch repair, we prepared heteroduplex DNAs that contained a G·T mismatch (A·T base pair in control DNAs), one hemimodified d(GATC) sequence, and 0, 1, or 2 EcoRI-recognition sequences (Fig. 1*A*; see Fig. 3).

Effectiveness of a roadblock approach requires long-term occupancy of the roadblock site. As judged by filter-binding assay, the $t_{1/2}$ for dissociation of $EcoRI_{E111Q}$, from plasmid pBR322 in 0.15 M NaCl in the absence of Mg^{2+} is ≈550 min, but this value is expected to be reduced ≈3-fold in the presence of

Author contributions: A.P. and P.M. designed research; A.P. performed research; A.P. analyzed data; and A.P. and P.M. wrote the paper.

Conflict of interest statement: P.M. serves on the Scientific Advisory Board of Codon Devices; however, this paper is completely unrelated to his role in the company.

Freely available online through the PNAS open access option.

[§]To whom correspondence should be addressed. E-mail: modrich@biochem.duke.edu.

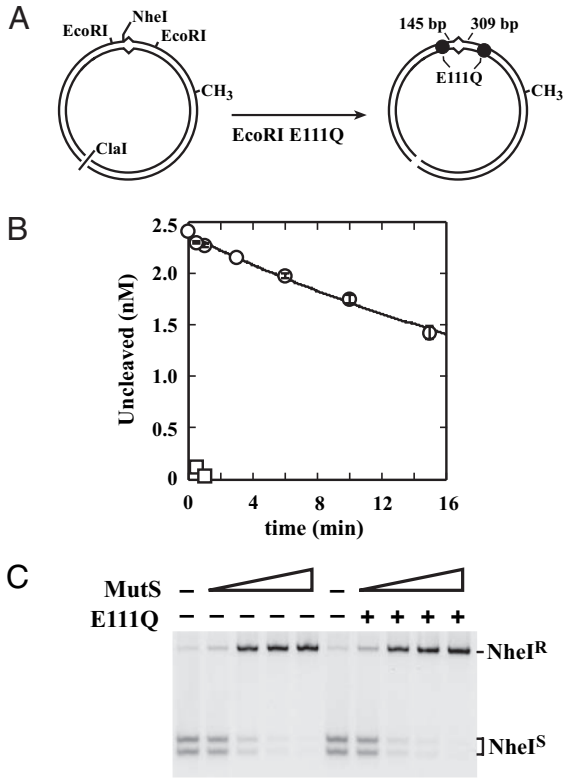

Fig. 1. Experimental system. (*A*) Heteroduplex DNAs contained a G·T mismatch, a single hemimodified d(GATC) site 1,024 bp from the mismatch, and EcoRI recognition sites at either, both, or neither of the positions indicated (see Fig. 3). One EcoRI site was located 309 bp from the mismatch, between the mispair and d(GATC) site (shorter path), and the second was located 145 bp to the other side of the mispair. Heteroduplexes also contained an NheI site 5 bp from the mismatch, which is rendered resistant to cleavage when MutS is bound to the mispair (12). Because the efficiency of MutH activation by MutS and MutL can be affected by superhelical density (9), circular substrates were linearized with ClaI before use to avoid experimental variability caused by possible differences in this parameter with different heteroduplex preparations. (*B*) ClaI linearized G·T heteroduplex (2.4 nM; two EcoRI sites) prebound with $EcoRI_{E111Q}$ (12 nM) was challenged with 120 nM WT EcoRI endonuclease, and the reaction was sampled to score the remaining intact DNA (circles) (see *Materials and Methods*). Error bars are ±1 SD (three determinations). The curve shown was determined by nonlinear least-squares fit to a single exponential (amplitude, 2.36 nM; $k = 0.0311\ min^{-1}$; $R^2 = 0.991$). Because the heteroduplex contained two EcoRI sites, the rate of cleavage per site is half of that shown. (No preferential cleavage of either site was observed.) The two-EcoRI-site heteroduplex also was challenged with 120 nM EcoRI in the absence of $EcoRI_{E111Q}$; the intact heteroduplex was not detectable after 30 s of reaction, but low levels of molecules that cleaved at just one site or the other were observed (squares). (*C*) Reactions containing 2.4 nM G·T heteroduplex with two EcoRI sites (prebound as indicated with 24 nM $EcoRI_{E111Q}$) were supplemented with 0, 12.5, 25, 50, or 100 nM MutS as the monomer. After 15 min at 37°C, samples of the reactions were challenged with NheI for 1 min. The challenge of samples from the same reaction with WT EcoRI demonstrated that >95% of EcoRI sites were occupied by $EcoRI_{E111Q}$ (data not shown).

the divalent cation (19, 20). However, this lifetime does not necessarily correspond to the residency time of the protein at an EcoRI site. Because EcoRI locates and leaves its recognition site by facilitated diffusion (21), endonuclease–DNA complexes that score positively by filter-binding assay include those in which the endonuclease has left and returned to the recognition site by diffusion within the polynucleotide domain. To obtain a better estimate of $EcoRI_{E111Q}$ residency time, a heteroduplex containing two EcoRI sites was prebound with $EcoRI_{E111Q}$ [2.5 dimers per d(GAATTC) sequence] (Fig. 1*A*), and the $EcoRI_{E111Q}$–DNA complexes were then challenged with an excess of WT EcoRI endonuclease (25 dimers per recognition site). Under these conditions, >95% of the heteroduplex molecules were protected from cleavage by the bound $EcoRI_{E111Q}$, but the extent of this protection decreased with time, with a $t_{1/2}$ of 20 min per heteroduplex, or 40 min per EcoRI site (Fig. 1*B*). Although kinetic competition experiments (data not shown) indicate that $EcoRI_{E111Q}$ and WT EcoRI achieve recognition of a d(GAATTC) sequence with comparable efficiency, the challenge experiment of Fig. 1*B* overestimates the $EcoRI_{E111Q}$ residency time. This is because complications attributable to EcoRI* activity precluded the use of higher challenge concentrations of WT endonuclease. Furthermore, a challenge assay of this type is expected to be inefficient with respect to scoring transient microscopic dissociation events because a site-specific binding protein will have an extremely high probability of returning to its recognition site (22). Based on such arguments, we conclude that the residency half-life of $EcoRI_{E111Q}$ at a d(GAATTC) sequence is less than the 40 min value estimated above.

The possibility that heteroduplex-bound $EcoRI_{E111Q}$ might interfere with mismatch recognition by MutS also was tested. The heteroduplexes used in these experiments contain an NheI site 5 bp from the mismatch, which is rendered resistant to cleavage by MutS binding (12). As shown in Fig. 1*C*, MutS recognition of the G·T mismatch was unaffected by heteroduplex-bound $EcoRI_{E111Q}$.

$EcoRI_{E111Q}$ Inhibits Mismatch-Dependent MutH Activation. Initiation of *E. coli* mismatch repair involves the mismatch-, MutS-, MutL- and ATP-dependent activation of MutH endonuclease, which incises the unmethylated strand at a hemimethylated d(GATC) site (9). Because the unmodified d(GATC) sequence that is subject to incision may reside either 3′ or 5′ to the mismatch, heteroduplexes are assigned a polarity according to 3′ or 5′ placement of this sequence relative to the mispair (9). For circular heteroduplexes, this polarity refers to the shorter path between the two sites.

We initially tested the influence of $EcoRI_{E111Q}$ roadblocks (five dimers per EcoRI site) on the kinetics of mismatch-, MutS-, and MutL-dependent MutH activation by using 5′ or 3′ G·T heteroduplexes (or A·T homoduplexes) that contained a mismatch bounded on either side by an EcoRI recognition site (Fig. 1*A*). Because this reaction responds to superhelical density of closed circular heteroduplexes, circular substrates were linearized with ClaI before use to avoid experimental differences caused by this variation in this parameter with different heteroduplex preparations (9). A marked reduction in the efficiency of MutH activation was observed with both 5′ and 3′ heteroduplexes when the DNAs contained prebound $EcoRI_{E111Q}$, as compared with mock-prebound substrates (Fig. 2). As judged by initial rates during the first minute of reaction, $EcoRI_{E111Q}$ roadblocks reduced the efficiency of MutH activation on the 5′ heteroduplex by 72% and that on the 3′ heteroduplex by 56% (Table 1). However, as can be seen in Fig. 2 and Table 1, homoduplex control DNAs that were prebound with $EcoRI_{E111Q}$ also were subject to a limited but significant level of MutH incision under these experimental conditions. When corrected for this background incision, the degree of $EcoRI_{E111Q}$ inhibition was 81% for 5′ and 72% for 3′ heteroduplexes.

To further clarify the basis of these $EcoRI_{E111Q}$ effects, we examined effects of the protein on MutH activation by using 3′ heteroduplexes that contained only one of the two EcoRI sites in the DNAs described above or that lacked an EcoRI site altogether. Significant inhibition by $EcoRI_{E111Q}$ only occurred when the heteroduplex contained an EcoRI site between the mismatch and the d(GATC) sequence within the linear substrate (Fig. 3 and Table 1).

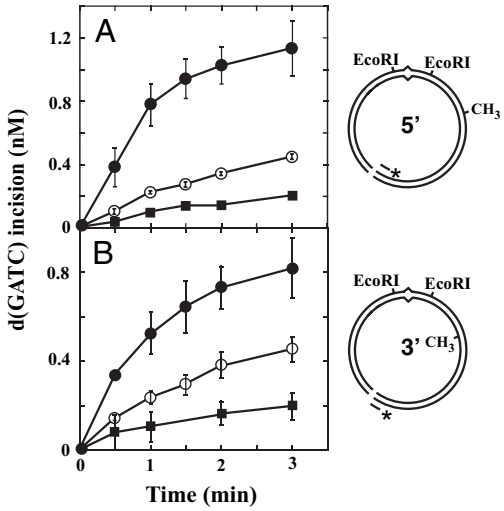

Fig. 2. $EcoRI_{E111Q}$ inhibits MutH activation on a linear G·T substrate. (*A*) Covalently closed circular 5′ G·T heteroduplex or A·T homoduplex DNAs containing two EcoRI sites were linearized with ClaI (Fig. 1*A*), prebound with $EcoRI_{E111Q}$ as indicated, and then incubated with MutH, MuL, MutS, and ATP (see *Materials and Methods*). Reactions were sampled as a function of time and were quenched, and products were resolved by electrophoresis through alkaline agarose and transferred to a nitrocellulose membrane. The substrate and product were visualized by hybridization with an excess of the ^{32}P-5′-end-labeled oligonucleotide V2505 (see schematic at right), which hybridizes to the unmethylated strand. The 2,313-nucleotide segment resulting from d(GATC) incision was quantitated by using a phosphorimager. Filled circles, G·T heteroduplex in the absence of $EcoRI_{E111Q}$ (mock prebound); open circles, G·T heteroduplex prebound with $EcoRI_{E111Q}$; squares, A·T homoduplex prebound with $EcoRI_{E111Q}$. Error bars are ±1 SD (three determinations). (*B*) Experimental procedure and symbols are as in *A*, but DNA substrates were 3′ G·T heteroduplex or A·T homoduplex DNAs. Incision at the d(GATC) site was scored by hybridization with ^{32}P-5′-end-labeled oligonucleotide C2527, which hybridizes to the unmethylated strand.

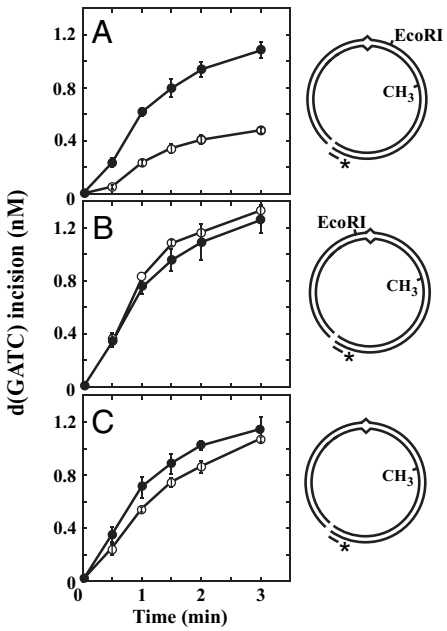

Fig. 3. $EcoRI_{E111Q}$ inhibition of MutH activation depends on EcoRI site location. (*A*) MutHLS reactions on 3′ G·T heteroduplex DNAs. The descriptions of the symbols are the same as for those in Fig. 2*B*, except that DNAs contained one or no EcoRI site, as indicated. The individual EcoRI sites present in the molecules shown in *A* and *B* correspond to the two sites present in the DNAs shown in Fig. 2. The error bars indicate the SD for three independent experiments (*A*) or the range of values observed in two independent experiments (*B* and *C*).

A Double-Strand Break Between the Mispair and the d(GATC) Site Abolishes MutH Activation. As an alternate approach to distinguish models that invoke DNA looping or signaling along the helix contour to account for mismatch–d(GATC) interaction during mismatch repair, we have introduced a double strand break at various points in the circular heteroduplexes that are used to score the reaction *in vitro*. Although a strategically placed helix disruption is expected to abolish MutH activation if events leading to this effect involve signaling along the helix contour, effects on mismatch–d(GATC) site interaction attributable to DNA looping are expected to be more limited. To test this hypothesis, we prepared sets of circularly permuted linear substrates by linearization of covalently closed circular 3′ or 5′ heteroduplexes with a set of single cutting restriction enzymes. As shown in Fig. 4, endonucleases that cleaved the circular molecules within a longer path (5,400 bp) linking the mismatch and d(GATC) site yielded linear molecules that were excellent substrates for MutH activation. By contrast, introduction of a double strand break within the shorter path (1,000 bp) linking the two sites dramatically attenuated the reaction. The initial rate of MutH incision during the first minute of reaction was undetectable (<5% of that observed with linear substrates produced by cleavage within the longer path).

Table 1. Rates of MutH activation

Heteroduplex	Location of EcoRI site(s)		d(GATC) cleavage, fmol/min	
	Short path	Long path	Without $EcoRI_{E111Q}$	With $EcoRI_{E111Q}$
5′ G·T	+	+	7.7 ± 1.6	2.1 ± 0.2
3′ G·T	+	+	5.9 ± 1.0	2.6 ± 0.3
3′ G·T	+	−	5.7 ± 0.8	2.1 ± 0.8
3′ G·T	−	+	7.5 ± 0.5	8.1 ± 0.9
3′ G·T	−	−	6.9 ± 0.7	5.3 ± 0.6
5′ A·T	+	+	—	0.8
3′ A·T	+	+	—	1.3 ± 0.8

Initial rates of MutH incision were determined from the experiments of Figs. 2 and 3 during the first minute of reaction. When indicated, results shown are ±1 SD. The values shown are not corrected for background incision observed on control A·T homoduplex DNAs.

Discussion

As discussed above, three types of model have been proposed to account for mismatch–d(GATC)–strand signal interaction during *E. coli* methyl-directed mismatch repair. Two of these models invoke signaling along the DNA contour between the two DNA sites via repair activity movement or polymerization along the helix (11). Evidence for ATP-dependent movement of MutS and the MutS–MutL complex along the helix is available (12, 13), but the function of this movement in mismatch repair has not been established. The third model stipulates that the MutS–MutL complex remains bound to the mismatch and activates MutH at a d(GATC) sequence by a mechanism in which the two sites are brought into proximity by DNA looping (14, 15). As discussed above, a key feature of methyl-directed mismatch repair is its bidirectional capability: MutH incision at an unmethylated d(GATC) sequence located either 3′ or 5′ to the mismatch is followed by loading of the appropriate 3′-to-5′ or 5′-to-3′ excision system at the ensuing strand break (2–4, 10). Although models that invoke signaling along the helix can account, in principle, for this orientation-dependent response, the DNA-

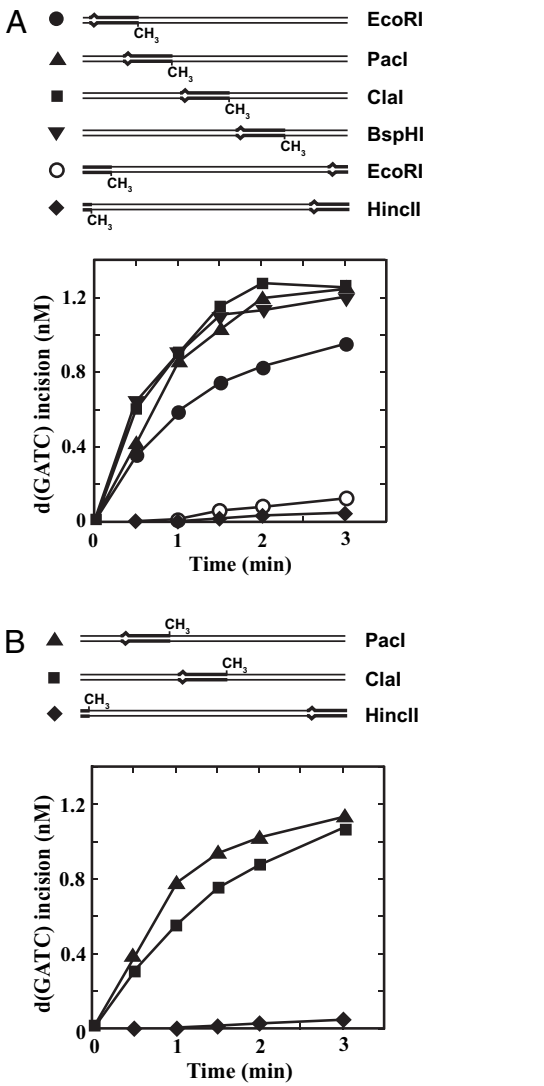

Fig. 4. Effects of a helix discontinuity on MutH activation. (*A*) Closed circular 3′ G·T heteroduplexes were linearized with individual endonucleases as indicated and then subjected to treatment with MutH, MutL, and MutS as described in Fig. 2. d(GATC) incision was scored after digestion with ClaI by hybridization with ^{32}P-5′-end-labeled oligonucleotide C2527 (oligonucleotide C2552 for the BspHI-linearized heteroduplex). The region encompassing the shorter path between the mismatch and the d(GATC) site in the circular heteroduplex is shown in bold. (*B*) The analysis of d(GATC) incision after restriction enzyme linearization was as in *A*, except that 5′ heteroduplexes were used.

looping model has not yet been reconciled with the bidirectional nature of the reaction because it is not clear how such a mechanism would support establishment of the orientation of the two DNA sites, a requirement for loading the correct excision system.

The results presented here demonstrate that an EcoRI$_{E111Q}$ protein roadblock placed between the mismatch and the d(GATC)-strand signal inhibits MutH activation by 70–80%, results that are most readily interpreted in terms of a mechanism in which MutH activation depends on signaling along the DNA helix. Although inhibition in this system is incomplete, EcoRI$_{E111Q}$ cannot be regarded as an absolute roadblock because it leaves its recognition site at a significant rate, for which we are able to estimate only a lower limit (residency $t_{1/2} < 40$ min). It therefore seems likely that the EcoRI$_{E111Q}$-insensitive events are attributable, at least in part, to diffusion of the mutant endonuclease away from its recognition site. Nevertheless, our EcoRI$_{E111Q}$ results do not exclude the possibility that a small fraction of MutH activation events depend on a mechanism that involves DNA looping. It also is pertinent to note in this regard that sequence recognition by EcoRI confers a 50° bend on the helix (23). Although a fixed bend can alter the torsional alignment of two DNA sites that is necessary for an activation mechanism based on DNA looping, such effects are expected to be nonexistent or nearly so when the separation distance exceeds 800 bp (24), as is the case in the experiments described here.

We have also found that a double-strand break within the 1,000-bp shorter path linking the mismatch and the single d(GATC) site in a 6,400-bp circular heteroduplex essentially abolishes MutH activation, whereas a double-strand break placed within the longer path is without effect. These findings are extremely difficult to reconcile with a DNA-looping mechanism for MutH activation. The likelihood that two DNA segments within a given molecule will be in proximity can be estimated from the ring closure probability, or j factor (24), which has been experimentally evaluated by Baldwin and colleagues (25). Although the probability that two sites separated by 1,000 bp will diffuse into proximity is greater than that for two sites separated by 5,400 bp, these values differ by less than a factor of 4 (25). This difference is much less than the rate disparity (>20-fold) observed for MutH activation on linear heteroduplexes in which the mismatch and d(GATC) separation distance is 1,000 bp as compared with that for molecules in which the two sites are separated by the longer distance (Fig. 4). Coupled with EcoRI$_{E111Q}$ roadblock results, the strong dependence of the efficiency of MutH activation on mismatch–d(GATC) separation distance, as measured along the DNA backbone, provides a compelling argument that the initiation of *E. coli* mismatch repair involves signaling along the helix contour. This suggestion also is consistent with findings in several laboratories that *in vitro* and *in vivo* repair efficiencies for circular heteroduplexes decrease with increasing separation distance of the mismatch and a hemimethylated d(GATC) site (26–28).

This conclusion differs from that of Wang and Hays (29), who found that placement of a streptavidin–biotin complex between the mismatch and strand signal to be without effect on the initiation of mismatch-provoked excision in nuclear extracts of human cells. There are several possible explanations for these differing results and conclusions. Because the streptavidin complex used by Wang and Hays (29) was offset from the helix by a 15-carbon linker and could have been subject to displacement by extract activities, its presence may not have represented an effective barrier to a signaling event propagating along the DNA. However, these differing results could also be indicative of fundamental differences in the mechanisms of *E. coli* and human mismatch repair. In fact, recent analysis of human MutLα has suggested that the *E. coli* and human mismatch repair reactions may differ significantly in this regard. In contrast to *E. coli* MutL, which is believed to couple mismatch recognition by MutS to the activation of downstream activities including the excision system (10, 30), human MutLα has been shown to be a latent endonuclease that is activated in a mismatch-, MutSα-, replication factor C-, and proliferating cell nuclear antigen-dependent manner (31). Attempts to detect endonuclease activity associated with *E. coli* MutL have yielded negative results (F. A. Kadyrov, S. Holmes, M. Arana, O. A. Lukianova, M. O'Donnell, T. A. Kunkel, and P. Modrich, unpublished data).

Materials and Methods

DNAs and Proteins. EcoRI sites were introduced into bacteriophages f1MR1 and f1MR3 (32) by oligonucleotide mutagenesis. An AATT sequence was introduced between positions 5491 and 5492 of f1MR1 and f1MR3 to yield f1MR61 and f1MR62,

respectively, thus yielding a GAATTC site. The four-nucleotide insertion alters the two C-terminal amino acids of the f1 gene IV product and adds five additional residues to the protein but is without significant effect on phage viability. Phages f1MR63 and f1MR64 were constructed from f1MR1 and f1MR3 by T-to-C substitution at position 5950 within the intergenic region to convert a GAATTT sequence to an EcoRI site. Phages f1MR65 and f1MR66 containing two EcoRI sites at positions 5491 and 5945 were constructed by restriction fragment swaps between f1MR61 and f1MR63 and between f1MR62 and f1MR64. All mutant derivatives were confirmed by sequence analysis. Hemimethylated closed circular heteroduplexes and control homoduplex DNAs contained a G·T mismatch or A·T base pair at position 5632 (5636 when the EcoRI site at 5491 was present) and a single hemimethylated d(GATC) site at position 216 that was 1,024 bp from the mismatch either on the complementary (3′ heteroduplex) or viral DNA strand (5′ heteroduplex) (Fig. 1). The substrates contained one or two EcoRI sites, as indicated, and were prepared as described previously (32). Linear DNAs were prepared by digestion of the circular substrates with an appropriate restriction endonuclease, followed by phenol extraction and ethanol precipitation.

MutS (33), MutL (34), MutH (35), EcoRI (36), and $EcoRI_{E111Q}$ (19) were purified by published methods. ClaI, HincII, PacI, and BspHI were obtained from commercial sources.

Binding of $EcoRI_{E111Q}$. Reactions (8 μl) contained 25 mM Tris·HCl (pH 7.4), 2.6 mM potassium phosphate, 144 mM KCl, 0.01 mM EDTA, 1.4 mM DTT, 126 μg/ml BSA, 0.6% glycerol, 6.25 mM $MgCl_2$, 2.5 mM ATP, 3 nM linear heteroduplex or homoduplex DNA, and 30 nM hydrolytically defective $EcoRI_{E111Q}$ (as dimer). Incubation was at 0°C for 30 min followed by 5 min at 37°C. Mock reactions were performed in the absence of $EcoRI_{E111Q}$.

EcoRI site occupancy by $EcoRI_{E111Q}$ was scored by challenge with excess WT endonuclease. Scaled-up binding reactions (56 μl) contained 3 nM linear heteroduplex (two EcoRI sites) and 15 nM $EcoRI_{E111Q}$. After incubation as described above, the reactions were challenged by addition of 14 μl of 600 nM WT EcoRI. Samples (10 μl) were withdrawn as a function of time, and hydrolysis was terminated by addition of 90 μl of 22 mM EDTA followed by phenol extraction and ethanol precipitation. DNA products were electrophoresed through 1% agarose gels, and the extent of cleavage was determined by using a photometric grade CCD camera (Photometrics, Tucson, AZ) after ethidium bromide staining.

MutS-Binding Reactions. Binding of MutS to heteroduplex was scored by NheI-resistance assay (12). Reactions (20 μl) contained 20 mM Tris·HCl (pH 7.4), 6 mM potassium phosphate, 55 mM KCl, 0.03 mM EDTA, 1 mM DTT, 300 μg/ml BSA, 0.5% glycerol, 5 mM $MgCl_2$, 2.4 nM linear heteroduplex (prebound with 24 nM $EcoRI_{E111Q}$ or mock prebound), and MutS as indicated. Because of the sensitivity of NheI to high ionic strength, the reactions used a lower KCl concentration than that used for the MutH-activation assays. After incubation at 37°C for 15 min, 10 μl of samples were supplemented with 10 units of NheI in 5 μl of reaction buffer (to score for MutS binding) or with 96 nM EcoRI in 5 μl of reaction buffer (to score for $EcoRI_{E111Q}$ binding). Incubation was continued for another 60 or 30 s after NheI or EcoRI treatment, respectively. Hydrolysis was quenched, and cleavage was scored as described above.

MutH-Activation Reactions. Incision at the single hemimethylated d(GATC) site by activated MutH (9) was performed under conditions of the MutS-binding reactions described above, except that KCl concentration was increased to 125 mM and that ATP was present at 2 mM. Reactions (70 μl) contained 2.4 nM heteroduplex (prebound with 24 nM $EcoRI_{E111Q}$ or mock-prebound), 37 nM MutS, 25 nM MutL, and 5 nM MutH (expressed as monomer equivalents). Incubation was at 37°C, and samples (10 μl) were removed as indicated and quenched as described above. Incision at the d(GATC) site was scored by indirect end labeling. Products of the reaction were resolved by electrophoresis through 1% alkaline agarose, transferred to a Hybond-XL membrane (Amersham, Piscataway, NJ) after depurination and strand breakage to ensure effective transfer of large fragments (37), and hybridized with an excess of ^{32}P-5′-end-labeled oligonucleotide probes V2505 [d(CGCTACTGATTACGGTGCTGCT)], C2527 [d(AGCAGCACCGTAATCAGTAGCG)], or C2552 [d(GAAACGTCACCAATGAAACCAT)]. Probe V2505 hybridizes to the complementary strand adjacent to the ClaI site and was used to map incision on the 5′ substrate. Probes C2527 or C2552 hybridized to the viral strand adjacent to the ClaI and were used to map incision on the 3′ substrates. In all cases, these probes hybridized to the strand that contained the unmethylated d(GATC) sequence. Results were quantitated by using a Typhoon phosphorimager and ImageQuant version 5.2 software (GE Healthcare, Piscataway, NJ).

This work was supported in part by National Institutes of Health Grant GM23719. P.M. is an Investigator of the Howard Hughes Medical Institute.

1. Lahue RS, Au KG, Modrich P (1989) *Science* 245:160–164.
2. Cooper DL, Lahue RS, Modrich P (1993) *J Biol Chem* 268:11823–11829.
3. Burdett V, Baitinger C, Viswanathan M, Lovett ST, Modrich P (2001) *Proc Natl Acad Sci USA* 98:6765–6770.
4. Viswanathan M, Burdett V, Baitinger C, Modrich P, Lovett ST (2001) *J Biol Chem* 276:31053–31058.
5. Meselson M (1988) in *Recombination of the Genetic Material*, ed Low KB (Academic, San Diego), pp 91–113.
6. Su SS, Modrich P (1986) *Proc Natl Acad Sci USA* 83:5057–5061.
7. Grilley M, Welsh KM, Su SS, Modrich P (1989) *J Biol Chem* 264:1000–1004.
8. Galio L, Bouquet C, Brooks P (1999) *Nucleic Acids Res* 27:2325–2331.
9. Au KG, Welsh K, Modrich P (1992) *J Biol Chem* 267:12142–12148.
10. Dao V, Modrich P (1998) *J Biol Chem* 273:9202–9207.
11. Modrich P (1987) *Annu Rev Biochem* 56:435–466.
12. Allen DJ, Makhov A, Grilley M, Taylor J, Thresher R, Modrich P, Griffith JD (1997) *EMBO J* 16:4467–4476.
13. Acharya S, Foster PL, Brooks P, Fishel R (2003) *Mol Cell* 12:233–246.
14. Junop MS, Obmolova G, Rausch K, Hsieh P, Yang W (2001) *Mol Cell* 7:1–12.
15. Schofield MJ, Nayak S, Scott TH, Du C, Hsieh P (2001) *J Biol Chem* 276:28291–28299.
16. Kunkel TA, Erie DA (2005) *Annu Rev Biochem* 74:681–710.
17. Iyer RR, Pluciennik A, Burdett V, Modrich PL (2006) *Chem Rev* 106:302–323.
18. Jiricny J (2006) *Nat Rev Mol Cell Biol* 7:335–346.
19. Wright DJ, King K, Modrich P (1989) *J Biol Chem* 264:11816–11821.
20. King K, Benkovic SJ, Modrich P (1989) *J Biol Chem* 264:11807–11815.
21. Wright DJ, Jack WE, Modrich P (1999) *J Biol Chem* 274:31896–31902.
22. Berg OG, Winter RB, von Hippel PH (1981) *Biochemistry* 20:6929–6948.
23. Thompson JF, Landy A (1988) *Nucleic Acids Res* 16:9687–9705.
24. Rippe K, von Hippel PH, Langowski J (1995) *Trends Biochem Sci* 20:500–506.
25. Shore D, Langowski J, Baldwin RL (1981) *Proc Natl Acad Sci USA* 78:4833–4837.
26. Bruni R, Martin D, Jiricny J (1988) *Nucleic Acids Res* 16:4875–4890.
27. Lahue RS, Su SS, Modrich P (1987) *Proc Natl Acad Sci USA* 84:1482–1486.
28. Lu, AL (1987) *J Bacteriol* 169:1254–1259.
29. Wang H, Hays JB (2004) *EMBO J* 23:2126–2133.
30. Hall MC, Matson SW (1999) *J Biol Chem* 274:1306–1312.
31. Kadyrov FA, Dzantiev L, Constantin N, Modrich P (2006) *Cell* 126:297–308.
32. Su SS, Lahue RS, Au KG, Modrich P (1988) *J Biol Chem* 263:6829–6835.
33. Blackwell LJ, Bjornson KP, Allen DJ, Modrich PL (2001) *J Biol Chem* 276:34339–34347.
34. Spampinato C, Modrich P (2000) *J Biol Chem* 275:9863–9869.
35. Welsh KM, Lu AL, Clark S, Modrich P (1987) *J Biol Chem* 262:15624–15629.
36. Cheng SC, Kim R, King K, Kim SH, Modrich P (1984) *J Biol Chem* 259:11571–11575.
37. Dzantiev L, Constantin N, Genschel J, Iyer RR, Burgers PM, Modrich P (2004) *Mol Cell* 15:31–41.